


 Cite this: *Chem. Commun.*, 2021, 57, 9466

 Received 18th June 2021,
 Accepted 16th August 2021

DOI: 10.1039/d1cc03248h

rsc.li/chemcomm

Carborane photochromism: a fatigue resistant carborane switch†‡

 Chong Li,^{id}*^a Matthew P. Aldred,^{id}^a Rachel A. Harder,^b Ying Chen,^a
 Dmitry S. Yufit,^{id}^b Ming-Qiang Zhu^{id}^a and Mark A. Fox^{id}*^b

A dithienylethene molecule involving carborane clusters shows remarkable fatigue resistance and high contrast visual colour changes when irradiated with alternating ultraviolet and visible light. The fluorescence of this assembly can be switched on and off when irradiated in the solid state but not in the solution state.

Photochromism is the reversible transformation of a chemical species between two forms by the absorption of electromagnetic radiation, where the two forms have different absorption spectra.^{1–5} Single molecule switches due to photochromism are highly desirable as components of molecular electronics especially in recording media applications.^{6–11} Such switches must have non-destructive readout capability for applications and the dithienylethene (DTE) derivatives (Fig. 1) are among the most promising switches with outstanding fatigue-resistant photochromic performances.^{12–14} DTE photochromism is P-type, in which the open form of DTE converts to the closed form under UV radiation and under visible light the closed form returns to the open form.^{14–18}

Carboranes are clusters of boron, carbon and hydrogen atoms with *ortho*-carborane derivatives as the most researched carboranes for two main reasons, firstly being easily synthesised from various alkynes with commercially available decaborane and secondly these carboranes have been intensively investigated recently for their diverse and unusual photophysics.^{19–32} Here we describe carborane

photochromism for the first time by synthesising the carborane DTE photoswitch **2** in one step from the corresponding alkynyl DTE photoswitch **1** with decaborane (Fig. 2). Unlike the alkynyl analogue **1**, the carborane DTE photoswitch **2** exhibits fatigue-resistant photochromic properties.

The alkynyl photoswitch **1** was isolated as a light blue solid as the open form with the coloured closed DTE form present in minor amount. The carborane DTE switch **2** was synthesised as a white solid from **1** and decaborane in 56% yield with the lack of colour indicating an open DTE form with a negligible amount of closed form. The open forms of **1** and **2** were confirmed by X-ray crystallography as anti-parallel conformers (Fig. 3).

The colours of the carborane DTE switch **2** are beneficial as applying UV radiation to the white solid resulted in a high contrast colour change from white to purple (Fig. 4). The colour of **2** reverses from purple to white under white light thus **2** is an excellent photoswitch. The colour of the alkynyl DTE photoswitch **1** also changed from light blue to purple but was found to decompose during UV irradiation based on the NMR data of the closed form (Fig. S4, ESI†).

A dithienylethene (DTE) core generally does not exhibit any luminescence behaviour. Adding a fluorophore (or π -conjugated systems) around the DTE core is frequently employed to facilitate fluorescence photoswitching. Conventional fluorophores such as perylenes,^{33–35} naphthalimides,³⁶ BODIPY,³⁷ tetraphenylethene^{38,39} and rhodamine,⁴⁰ have been attached to the DTE core for high-performance fluorescent photoswitches.⁴¹ It is noted that the outstanding performances of these switches are demonstrated in the



Fig. 1 Photochromism of dithienylethene (DTE) derivatives.

^a Wuhan National Laboratory for Optoelectronics, School of Optical and Electronic Information, Huazhong University of Science and Technology, Wuhan, Hubei 430074, China

^b Department of Chemistry, Durham University, Lower Mountjoy, Stockton Road, Durham, DH1 3LE, UK

† Dedicated to Francesc Teixidor and Clara Viñas in celebration of their 70th birthdays. They have made so many contributions to the boron cluster chemistry community in the last 40 years including hosting EUROBORON and IMEBORON conferences.

‡ Electronic supplementary information (ESI) available: Experimental details for **1** and **2**, NMR, mass and IR spectra, photophysical and photoisomerisation details, cyclic voltammetry, crystallographic and computational data. CCDC 2070456 and 2070457. For ESI and crystallographic data in CIF or other electronic format see DOI: 10.1039/d1cc03248h



Communication



Fig. 2 DTE derivatives **1** and **2** discussed in this work. Each unlabelled vertex in the clusters is BH.

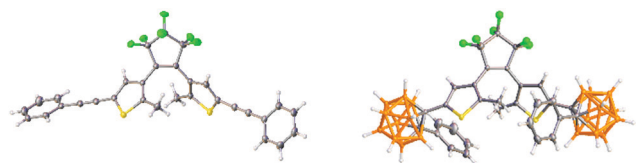


Fig. 3 Molecular structures for **1** (left) and **2** (right) determined by X-ray crystallography.



Fig. 4 Powder form of carborane photoswitch **2** taken under white light (right) and UV light (left). The length of time taken in seconds after UV irradiation (0.96 mW cm^{-2} , 302 nm) are given.

solvent states rather than in the solid states where such performances are expected to be lower. However, fluorescent photoswitch performances in the solid states are more suitable for practical applications.⁴² Here, fluorescence was found to be absent for **1** but present for **2** in the solid and solution states. In particular, compound **2** shows a superior fluorescence switching ability in the solid state which is an advantage over many reported DTE photoswitches.

When UV light is applied to the powdered form of **2**, the cyan fluorescence with a lifetime of 1 ns and a photoluminescence quantum yield (PLQY) of 0.5% is initially observed (Fig. 4). This fluorescence is switched off when UV radiation has converted the vast majority of the open forms to the closed forms so **2** can be considered as a fluorescent ON/OFF switch in the solid state. Similar photophysical data are shown when **2** is in alternative solid states in the form of a PMMA film or as solid aggregates in water (Fig. S22–S24, ESI†). The photoswitching property of the carborane DTE switch **2** showed excellent fatigue resistance in PMMA film (Fig. 5). The lowest energy band at 560 nm after UV irradiation of **2** is due to characteristic transitions involving the closed DTE unit leading to the intense purple colour corresponding to the closed form of **2**. The solid state fluorescence data for the open form of **2** with emission maxima of 474–497 nm (Fig. S19 and S27, ESI†) resemble that of 1-phenyl-2-(1'-pyridyl)-*ortho*-carborane with cyan colour emission maxima of 476 nm.²⁴ The open dithienylethene (DTE) unit thus plays a role akin to a heteroaryl group attached to a phenylcarborane cluster.

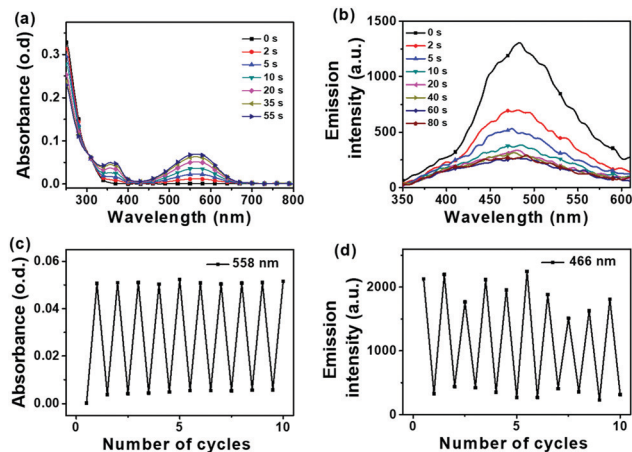


Fig. 5 (a) UV-Vis absorption spectra and (b) emission spectra of **2** in PMMA film upon 302 nm UV-light irradiation (0.96 mW cm^{-2}), showing the open-form to closed-form transition, at different time intervals, excitation wavelength = 320 nm . The photoswitching cycles of the (c) absorption and (d) fluorescence at maximum wavelength upon alternating UV-light (1.83 mW cm^{-2} , 302 nm) and visible-light (21.5 mW cm^{-2} , 621 nm) irradiations. Concentration = 5 wt% in PMMA.

In the three distinct solid states, the fluorescence spectra for the open forms of **2** are broad and have significant overlaps with the corresponding absorption spectra of closed forms of **2**. The fluorescence quenching in the closed form is mainly attributed to intramolecular energy transfer from the phenyl-carborane moiety to the closed DTE core moiety and, in the case of the aggregate and powdered forms, intermolecular energy transfers from the open forms of compound **2** to the neighbouring closed forms also result in fluorescence quenching.^{39,43–45} Such intermolecular energy transfers have been demonstrated in cyan fluorescence photoswitches.^{38,46–49}

Absorption data for **2** in solutions mirror the absorption spectra of the solid states for **2** before and after UV irradiation. The cluster switch **2** also showed remarkable ON/OFF fatigue resistance from photoswitching experiments in toluene (Fig. 6). While the alkyne **1** shows a photocyclisation quantum yield ($\Phi_{o \rightarrow c}$) of 41%, the carborane **2** shows a photocyclisation quantum yield of 100% (Table 1). Compound **2** appears to contain antiparallel conformations only (Fig. S38, ESI†) in the solution state, meaning that the absorbed light is quantitatively utilised for the ring closing reaction.^{50,51} A high photocyclisation quantum yield near 100% is rarely reported as most DTE derivatives such as **1** are limited to 50% as the parallel and antiparallel conformations are generally present in a 1:1 ratio in these DTE systems and only the anti-parallel conformations result in photocyclisations.⁴⁹ The observed $\Phi_{o \rightarrow c}$ values of **1** and **2** suggest that the sterics of the carborane clusters lead to exclusively antiparallel conformers in the open forms of **2** and thus provide a clear advantage in the photoswitching performance of **2** over **1** and other DTE derivatives.

The fluorescence spectra for **2** in solution differ from the emission spectra in the solid states where higher energy bands with vibronic structure at 412–465 nm (blue emission) are present in solution (Fig. 6). The fluorescence lifetime was 0.8



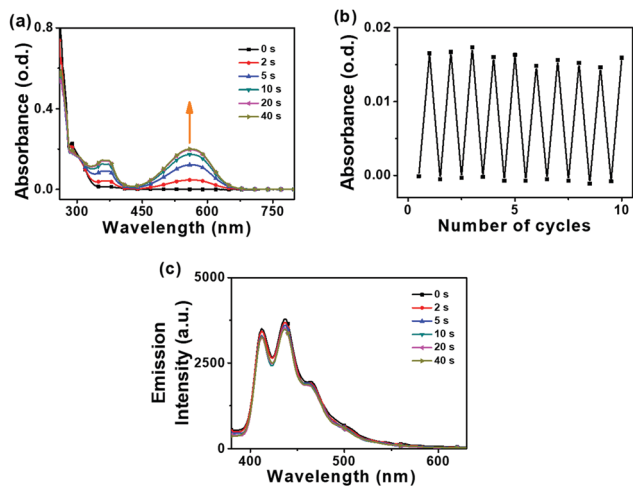


Fig. 6 (a) Absorption spectra of **2** in toluene solution (2×10^{-5} M) upon UV-light irradiation (0.96 mW cm^{-2}), (b) photo-switching cycles of the absorbance at λ_{max} (562 nm) of **2** upon alternating 302 nm UV-light (0.96 mW cm^{-2}) and 621 nm visible-light (21.5 mW cm^{-2}) irradiations, (c) emission spectra of **2** upon UV-light irradiation (0.96 mW cm^{-2}), concentration = 2.5×10^{-6} M.

Table 1 Photoisomerisation kinetic parameters and photoisomerisation quantum yields in toluene solution (2×10^{-6} M) for **1** and **2**

| | λ_{irr} [nm] | κ_{eq} | ε_{irr} [$\text{M}^{-1} \text{cm}^{-1}$] | α_{pss} | I [mW cm^{-2}] | κ_{ex} | $\Phi_{\text{o} \rightarrow \text{c}}$ or $\Phi_{\text{c} \rightarrow \text{o}}$ |
|-----------------------|--------------------------------|----------------------|--|-----------------------|--------------------------------|----------------------|---|
| Ring closing reaction | | | | | | | |
| 1 | 302 | 0.0928 | 52 750 | 0.79 | 0.591 | 0.55814 | 0.407 |
| 2 | 302 | 0.1568 | 9480 | 0.76 | 1.832 | 0.100307 | ~ 1 |
| Ring opening reaction | | | | | | | |
| 1 | 621 | 0.01842 | 27 278 | 0 | 7.684 | 1.966597 | 0.007 |
| 2 | 621 | 0.0329 | 6513 | 0 | 7.684 | 0.451724 | 0.055 |

λ_{irr} is the irradiation wavelength for photoisomerisation, the intensity of irradiation light is 0.591 or 1.832 mW cm^{-2} for 302 nm and 7.684 mW cm^{-2} for 621 nm. ε_{irr} is the molar extinction coefficient at wavelength λ_{irr} . α_{pss} is the fractional population of closed form in PSS irradiated under given wavelengths (obtained from the $^1\text{H-NMR}$ data, Fig. S28, ESI ‡). κ_{eq} is the rate constant of equilibration, which was fit with a monoexponential curve from the kinetics of re-equilibration from an arbitrary initial photostationary state (α_0) to a new photostationary state (α_{pss}). κ_{ex} is the excitation rate constant. Φ is the cyclisation ($\text{o} \rightarrow \text{c}$) or cycloreversion ($\text{c} \rightarrow \text{o}$) quantum yield.

ns and the PLQY was 0.2% for **2** in THF (Table S4, ESI ‡). Such emission bands appear to be generated from local excitations at the aryl groups and remain unaffected by the light and UV irradiation switching of the DTE unit. This is in contrast to the observed ON/OFF fluorescence switching of **2** in the solid state and thus different fluorescence pathways take place in the solid and solution states for **2**.

The weak blue fluorescence emissions observed for **2** in solutions (Fig. S27, ESI ‡) are not affected by quenching as the overlaps of the emission bands with the corresponding absorption spectra are poor. This lack of overlap results in negligible energy transfer so the real blue emissions in the solution states for **2** are not quenched upon UV irradiation.

Cyclic voltammetry (CV) measurements on the open form (Table S5, ESI ‡) of **2** reveal reduction waves at $E_{1/2}$ values of -1.64 and -1.72 V (vs. the ferrocenium/ferrocene couple) typical of two-electron reductions at the carborane cluster such as in 1-phenyl-2-(1'-pyridyl)-*ortho*-carborane (-1.55 and -1.67 V) 24 suggesting that the LUMO is at the carborane moiety. By contrast, the reduction waves in the CV trace for the closed form of **2** are not characteristic carborane waves with the irreversible first cathodic wave potential at -1.16 V compared to that of the open form of **2** at -1.84 V (Table S6, ESI ‡). Comparison with reported 52 CV reduction waves for DTE derivatives shows that the initial reduction takes place at the conjugated DTE unit in the closed form of **2** thus the LUMO of the DTE unit is involved in the low energy absorption bands observed for the closed form. This statement is supported by natural orbital analyses from hybrid DFT computations.

In conclusion, this study demonstrates that reversible carborane photochromism exists for the first time here. The carborane DTE switch has excellent ON/OFF fatigue resistance in the solid and solution states in contrast to the alkynyl analogue. More importantly, the carborane switch can also be a fluorescent ON/OFF switch in the solid states – a desirable property in recording media applications. The emission colours may be varied by replacing the phenyl groups with bulky fused-ring groups known to have novel emission properties therefore this study promises to start an exciting new field of unusual photochromic switches in material chemistry.

This work was supported by the National Natural Science Foundation of China (51603078, 22077037 and 51673077), the Fundamental Research Funds for the Central Universities (HUST: 2019kfyXKJC035). We also thank the Analytical and Testing Center of Huazhong University of Science and Technology, and the Center for Nanoscale Characterization & Devices (CNCD) of Wuhan National Laboratory for Optoelectronics (WNLO) for use of their facilities. We acknowledge EPSRC for a doctoral studentship (EP/P505186/1) and the High Performance Computing Service for access to a supercomputer (Hamilton) at Durham University.

Conflicts of interest

There are no conflicts to declare.

References

- M. Irie, T. Fukaminato, K. Matsuda and S. Kobatake, *Chem. Rev.*, 2014, **114**, 12174–12277.
- J. Zhang, Q. Zou and H. Tian, *Adv. Mater.*, 2013, **25**, 378–399.
- M. Irie, *Photochem. Photobiol. Sci.*, 2010, **9**, 1535–1542.
- K. Matsuda and M. Irie, *J. Photochem. Photobiol., C*, 2004, **5**, 169–182.
- M. Irie, *Chem. Rev.*, 2000, **100**, 1685–1716.
- T. Fukaminato, T. Doi, N. Tamaoki, K. Okuno, Y. Ishibashi, H. Miyasaka and M. Irie, *J. Am. Chem. Soc.*, 2011, **133**, 4984–4990.
- T. Fukaminato, *J. Photochem. Photobiol., C*, 2011, **12**, 177–208.
- T. Fukaminato, T. Umamoto, Y. Iwata, S. Yokojima, M. Yoneyama, S. Nakamura and M. Irie, *J. Am. Chem. Soc.*, 2007, **129**, 5932–5938.
- T. Fukaminato, T. Sasaki, T. Kawai, N. Tamai and M. Irie, *J. Am. Chem. Soc.*, 2004, **126**, 14843–14849.
- M. Irie, T. Fukaminato, T. Sasaki, N. Tamai and T. Kawai, *Nature*, 2002, **420**, 759–760.



- 11 C. Li, H. Yan, L.-X. Zhao, G.-F. Zhang, Z. Hu, Z.-L. Huang and M.-Q. Zhu, *Nat. Commun.*, 2014, **5**.
- 12 J. J. Zhang and H. Tian, *Adv. Opt. Mater.*, 2018, **6**, 1701278.
- 13 N.-H. Xie, C. Fan, H. Ye, K. Xiong, C. Li and M.-Q. Zhu, *ACS Appl. Mater. Interfaces*, 2019, **11**, 23750–23756.
- 14 M. Hanazawa, R. Sumiya, Y. Horikawa and M. Irie, *J. Chem. Soc., Chem. Commun.*, 1992, 206–207.
- 15 M. Irie and M. Mohri, *J. Org. Chem.*, 1988, **53**, 803–808.
- 16 M. Irie, S. Kobatake and M. Horichi, *Science*, 2001, **291**, 1769–1772.
- 17 M. Morimoto, S. Kobatake and M. Irie, *Adv. Mater.*, 2002, **14**, 1027–1029.
- 18 F. Terao, M. Morimoto and M. Irie, *Angew. Chem., Int. Ed.*, 2012, **51**, 901–904.
- 19 R. N. Grimes, *Carboranes*, Academic Press, Elsevier, New York, 3rd edn, 2016.
- 20 R. Núñez, M. Tarrés, A. Ferrer-Ugalde, F. F. de Biani and F. Teixidor, *Chem. Rev.*, 2016, **116**, 14307–14378.
- 21 J. Ochi, K. Tanaka and Y. Chujo, *Angew. Chem., Int. Ed.*, 2020, **59**, 2677–2680.
- 22 L. Weber, J. Kahlert, R. Brockhinke, L. Böhlting, A. Brockhinke, H.-G. Stammer, B. Neumann, R. A. Harder and M. A. Fox, *Chem. – Eur. J.*, 2012, **18**, 8347–8357.
- 23 K.-R. Wee, W.-S. Han, D. W. Cho, S. Kwon, C. Pac and S. O. Kang, *Angew. Chem., Int. Ed.*, 2012, **51**, 2677–2680.
- 24 L. Böhlting, A. Brockhinke, J. Kahlert, L. Weber, R. A. Harder, D. S. Yufit, J. A. K. Howard, J. A. H. MacBride and M. A. Fox, *Eur. J. Inorg. Chem.*, 2016, 403–412.
- 25 H. Naito, K. Nishino, Y. Morisaki, K. Tanaka and Y. Chujo, *Angew. Chem., Int. Ed.*, 2017, **56**, 254–259.
- 26 D. Tu, P. Leong, S. Guo, H. Yan, C. Lu and Q. Zhao, *Angew. Chem., Int. Ed.*, 2017, **56**, 11370–11374.
- 27 X. Wu, J. Guo, J. Zhao, Y. Che, D. Jia and Y. Chen, *Dyes Pigm.*, 2018, **154**, 44–51.
- 28 Z. Wang, T. Wang, C. Zhang and M. G. Humphrey, *ChemPhotoChem*, 2018, **2**, 369–379.
- 29 A. V. Marsh, N. J. Cheetham, M. Little, M. Dyson, A. J. P. White, P. Beavis, C. N. Warriner, A. C. Swain, P. N. Stavrinou and M. Heeney, *Angew. Chem., Int. Ed.*, 2020, **57**, 10640–10645.
- 30 A. Ferrer-Ugalde, A. González-Campo, C. Viñas, J. Rodríguez-Romero, R. Santillan, N. Farfán, R. Sillanpää, A. Sousa-Pedrares, R. Núñez and F. Teixidor, *Chem. – Eur. J.*, 2014, **20**, 9940–9951.
- 31 A. Ferrer-Ugalde, E. J. Juárez-Pérez, F. Teixidor, C. Viñas, R. Sillanpää, E. Pérez-Inestrosa and R. Núñez, *Chem. – Eur. J.*, 2012, **18**, 544–553.
- 32 L. Parejo, M. Chaari, S. Santiago, G. Guirado, F. Teixidor, R. Núñez and J. Hernando, *Chem. – Eur. J.*, 2021, **27**, 270–280.
- 33 M. Berberich, A.-M. Krause, M. Orlandi, F. Scandola and F. Würthner, *Angew. Chem., Int. Ed.*, 2008, **47**, 6616–6619.
- 34 C. Li, H. Yan, G.-F. Zhang, W.-L. Gong, T. Chen, R. Hu, M. P. Aldred and M.-Q. Zhu, *Chem. – Asian J.*, 2014, **9**, 104–109.
- 35 T. Fukaminato, T. Doi, N. Tamaoki, K. Okuno, Y. Ishibashi, H. Miyasaka and M. Irie, *J. Am. Chem. Soc.*, 2011, **133**, 4984–4990.
- 36 G. Jiang, S. Wang, W. Yuan, L. Jiang, Y. Song, H. Tian and D. Zhu, *Chem. Mater.*, 2006, **18**, 235–237.
- 37 T. A. Golovkova, D. V. Kozlov and D. C. Neckers, *J. Org. Chem.*, 2005, **70**, 5545–5549.
- 38 C. Li, W.-L. Gong, Z. Hu, M. P. Aldred, G.-F. Zhang, T. Chen, Z.-L. Huang and M.-Q. Zhu, *RSC Adv.*, 2013, **3**, 8967–8972.
- 39 C. Li, K. Xiong, Y. Chen, C. Fan, Y.-L. Wang, H. Ye and M.-Q. Zhu, *ACS Appl. Mater. Interfaces*, 2020, **12**, 27651–27662.
- 40 D. Xue, C. Zheng, S. Qu, G. Liao, C. Fan, G. Liu and S. Pu, *Luminescence*, 2017, **32**, 652–660.
- 41 C. Yun, J. You, J. Kim, J. Huh and E. Kim, *J. Photochem. Photobiol., C*, 2009, **10**, 111–129.
- 42 T. Nakagawa, Y. Miyasaka and Y. Yokoyama, *Chem. Commun.*, 2018, **54**, 3207–3210.
- 43 H. Wang, P. Zhang, B. P. Krishnan, M. Yu, J. Liu, M. Xue, S. Chen, R. Zeng, J. Cui and J. Chen, *J. Mater. Chem. C*, 2018, **6**, 9897–9902.
- 44 T. Fukaminato, S. Ishida and R. Métevier, *NPG Asia Mater.*, 2018, **10**, 859–881.
- 45 J. Su, T. Fukaminato, J.-P. Placial, T. Onodera, R. Suzuki, H. Oikawa, A. Brosseau, F. Brisset, R. Pansu, K. Nakatani and R. Métivier, *Angew. Chem., Int. Ed.*, 2016, **55**, 3662–3666.
- 46 S.-J. Lim, B.-K. An, S. D. Jung, M.-A. Chung and S. Y. Park, *Angew. Chem., Int. Ed.*, 2004, **43**, 6346–6350.
- 47 L. Ma, C. Li, Q. Yan, S. Wang, W. Miao and D. Cao, *Chin. Chem. Lett.*, 2020, **31**, 361–364.
- 48 R. Singh, H.-Y. Wu, A. K. Dwivedi, A. Singh, C.-M. Lin, P. Raghunath, M.-C. Lin, T.-K. Wu, K.-H. Wei and H.-C. Lin, *J. Mater. Chem. C*, 2017, **5**, 9952–9962.
- 49 N.-H. Xie, Y. Chen, H. Ye, C. Li and M.-Q. Zhu, *Front. Optoelectron.*, 2018, **11**, 317–332.
- 50 S. Fukumoto, T. Nakashima and T. Kawai, *Angew. Chem., Int. Ed.*, 2011, **50**, 1565–1568.
- 51 M. Takeshita, N. Kato, S. Kawauchi, T. Imase, J. Watanabe and M. Irie, *J. Org. Chem.*, 1998, **63**, 9306–9313.
- 52 W. R. Browne, J. J. D. de Jong, T. Kudernac, M. Walko, L. N. Lucas, K. Uchida, J. H. van Esch and B. L. Feringa, *Chem. – Eur. J.*, 2005, **11**, 6430–6441.

